Photocontrollable Crystallization at the Topological Defect of a Liquid Crystalline Droplet

Kenji Katayama (kkata@kc.chuo-u.ac.jp)
Chuo University https://orcid.org/0000-0003-3278-6485
Yota Sakai
Chuo University

Article

Keywords: Liquid crystalline droplet, Crystallization, Photo-induced phenomena

Posted Date: March 2nd, 2021

DOI: https://doi.org/10.21203/rs.3.rs-244385/v1

Photocontrollable Crystallization at the Topological Defect of a Liquid Crystalline Droplet

Yota Sakai[1] and Kenji Katayama[1]

1 Department of Applied Chemistry, Chuo University, Tokyo 112-8551, Japan;

*Corresponding author:

K. Katayama, Phone: +81-3-3817-1913, E-mail: kkata@kc.chuo-u.ac.jp

Abstract

Photo-controllable crystallization at the topological defect in an LC droplet was demonstrated. The dye molecules dissolved in a surfactant solution outside the LC droplet were promoted to move into the droplet by the light absorption. Nuclei emerged tens of seconds after light irradiation and moved toward the topological defect located at the droplet center, forming a branch-shaped crystal. This phenomenon was reproduced for three different dyes, and photo-induced migration, nucleation, and crystal formation were discussed as a possible mechanism.

Keywords: Liquid crystalline droplet; Crystallization, Photo-induced phenomena

Introduction

Crystallization of chemicals is a fundamental process for materials from the viewpoints of basic science and practical applications. In a well-established theory by La Mer,[1] an over-saturated solution starts to provide nuclei of a crystal at the initial stage, and subsequently, the nuclei grow in size as long as the concentration of the chemical is over-saturated. For practical purposes, crystallization is necessary for the pharmaceutical industry, and also it is vital in basic science for the determination of the molecular structure of chemicals and proteins by x-ray diffraction analysis (XRD). However, many chemicals cannot be crystallized due to fundamental reasons, such as solubility, chemical interaction, impurities, a short amount of chemicals, etc. Much effort has been made for crystallization by preparing over-saturated concentration via temperature, stirring speed, pH, etc,[2] and the technological progress has continued. For example, flow-based crystallization has been developed by control of anti-solvent and introduction of plug flow.[3–5] A unique technique, where the porous metal-organic framework has been demonstrated to absorb guest molecules and orient them in a crystalline form called as 'crystalline sponge method.' [6,7]

The liquid crystal (LC) is a phase between the solid and liquid, where it has a periodic structure in a specific direction like a crystal and has fluidity in another direction like a liquid, and this phase can be found frequently in living matter.[8] It plays a role in self-organization and structure formation for mechanical strength, color modification, and morphology, and also we can find it for display

purposes in our daily life. These days, topological defects in LCs have been paid much attention to because they could potentially control the structure and motion of LCs. The topological defect is an orientationally disordered point of LC molecules, where the molecular orientation cannot be defined. Intentionally formed topological defects by the photo-alignment layer could control the alignment of LCs and can be utilized for various thin optics.[9–11] When a droplet is formed with LC, different types of topological defects were formed inside and on the surface.[12] These droplets and spheres have been studied intensively as an 'active matter,' where the object could move around spontaneously like a living object by external energy sources. The motion of LC spheres was controlled by several topological defects, which also caused the self-assembly of molecules.[13] Topological defects were further investigated in biology because it was found that biological cells aligned like LC molecules and had topological defects. Furthermore, they could control the collective motion and biological activity depending on the types of defects.[14,15]

The defects in LCs sometimes could help to align and assemble colloids and molecules. Amphiphilic molecules were self-assembled to form nanostructures at the line defect (disclination).[13] LC ordering could align gold nanorods to the alignment direction in a lyotropic LC,[16] and also gold nanoparticles were concentrated at the dislocation of the smectic LC.[17,18] The force induced by the disclination line and colloids is regarded as a new type of force.[19] The defect-induced assembly was observed for dense colloid particles in LCs,[20], and the disclination was intentionally controlled to make

54 knots and links to form self-assembly of colloids.[21]

55 In this study, we accidentally found a unique crystallization phenomenon while studying a new
56 category of active matters consisted of LCs, which could move around in a surfactant solution due to
57 an induced convective flow inside and outside the droplets while gradually dissolving into it.[22–24] We
58 focused on the photo-controlled motion of the LC droplets by promoting adsorption and desorption of
59 molecules at the interface and could demonstrate the LC droplets approaching to and drawing away
60 from a light source,[25,26] and showed a clockwise/anti-clockwise rotation under the light.[27] During this
61 study, we found a crystallization of a chemical was triggered by light at the topological defect in a
62 pure LC droplet, even though the chemical was dissolved outside the LC droplet. Under the light
63 irradiation whose wavelength matches the absorption of chemicals, a crystal was formed inside an LC
64 droplet. It grew at the center of the droplet (topological defect) with a branched shape like an ice
65 crystal. This is the first demonstration of the topology-induced crystallization under the geometrical
66 frustration.[28] In this paper, we will show the demonstrations for the formation of several crystals and
67 describe the possible mechanism of this phenomenon.

68

69 # Result and discussions

70 Figure 1 shows an image sequence of a 5CB droplet surrounded by an SDS solution with *p*-
71 nitrophenol (0.01wt%) during the on-off operation of a UV light. The droplet had a topological defect

at the center, which is determined by the 5CB molecular alignment dominated by the boundary condition of the 5CB and the SDS solution (homeotropic alignment).[29] Surprisingly, we could recognize that small objects (~2 μm) started to nucleate inside the droplet about 30 s (Fig. 1(c)), and getting larger (Fig. 1(d)-(f)). Simultaneously, these objects were drawn into the center of the droplet, namely to the topological defect. The objects were gradually connected to grow and shaped branched structures. When the light was turned off, the small nucleated objects ceased to form gradually. These processes were repeated when the UV light was turned on again, and nucleated objects were connected to the original branches to make additional branches (Movie S1 in Supporting Information (SI)).

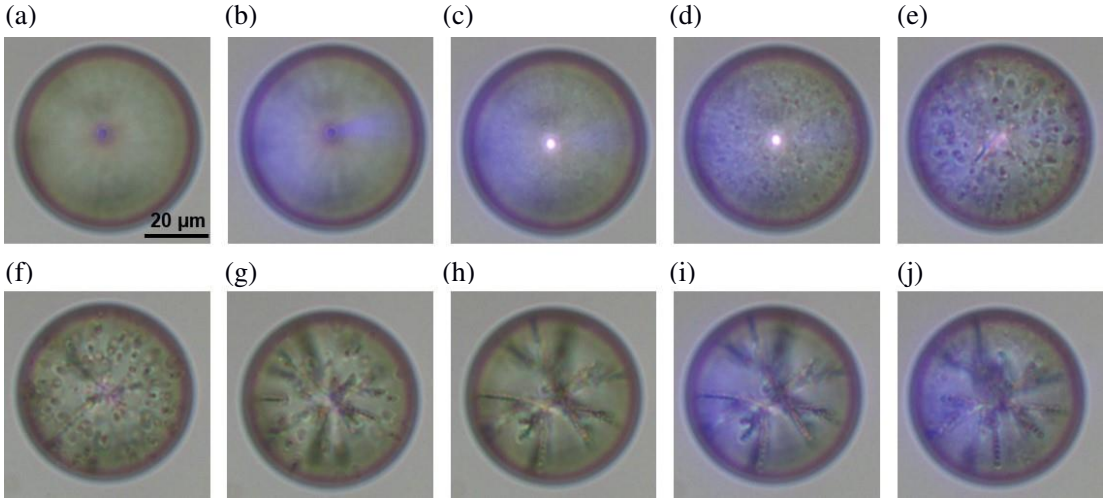

Fig.1 The snapshots of a 5CB droplet in an SDS solution with *p*-nitrophenol (0.01 wt%) under the on-off operation of the UV light is shown; (a) before irradiation, (b) - (e) 0, 30, 60 and 90 s after the UV was turned on, (f) - (h) 0, 60, and 120 s after the UV light was turned off, (i) and (j) 0 and 30 s after the UV light was turned on again.

This nucleation, growth and the subsequent structure formation inside the LC droplet was observed under the crossed-Nicole condition (Movie S2 in SI). Figure 2(a) and (b) show the snapshots

of the 5CB droplets before and after the nucleation and growth by irradiation of the UV light, respectively. Under the crossed-Nicole observation, the LC droplet showed a crossed texture (Fig.2(a)), known as a radial pattern, which indicates that the longer axis of molecules was oriented in the radial direction determined by the anchoring condition by the outside SDS molecules.[12,30] The generated branched-structure showed black lines along the branch direction, and each branch was sandwiched by whitish covers as shown in Fig.2(b). This result indicated that this object has polarization characteristics, suggesting the ordered alignment of molecules because the same color indicates the same orientation of the unit structure. It is supposed that the molecules are aligned either in the polarizer or analyzer direction in the black region, while they are in-between in the white regions. This result strongly suggests that the structured object was made of a crystalline state in which molecules were aligned in particular directions.

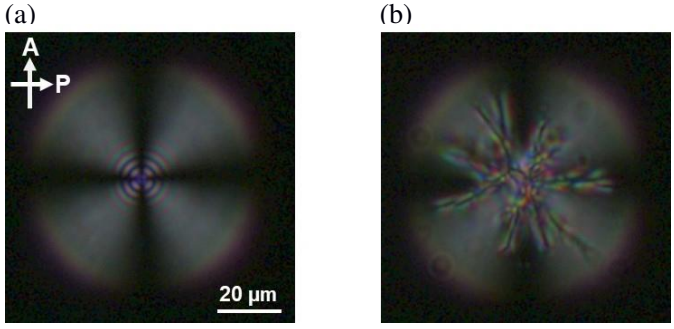

Fig.2 The snapshots of the 5CB droplet in an SDS solution with *p*-nitrophenol (0.01 %) observed by the polarization microscope under the crossed Nicole condition; (a) before irradiation (b) after the UV irradiation for 60 s. The white arrow in (a) indicates the direction of the analyzer and the polarizer.

These phenomena were observed for various dyes, and the results are shown in Fig. 3(a) and

103 (b) (Movie S3(a) and (b) in SI), corresponding for alizarin yellow GG and chrome yellow. We found
104 the nucleation, growth, and formation of the branched structure again for these molecules, and the
105 only difference was the formation speed of the branched structure. The necessary condition for these
106 phenomena was that the dyes need to have absorption at the wavelength of the illumination light, 365
107 nm. We did not observe the formation of objects for new coccine (λ_{max}~500 nm) and sunset yellow
108 (λ_{max}~480 nm), which do not have a major absorption band at the illumination light.

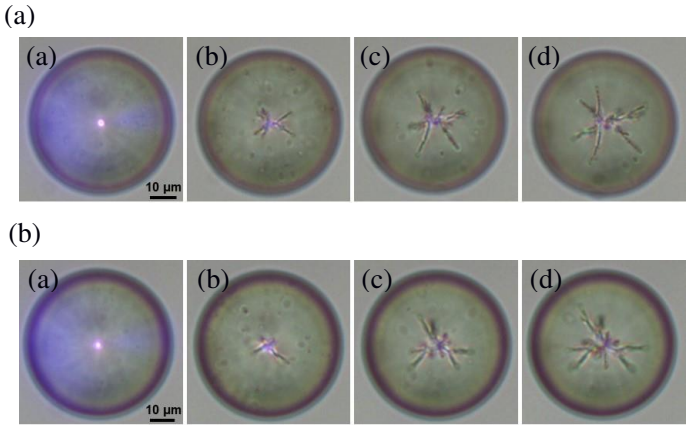

109 Fig.3 The snapshots of the 5CB droplet in an SDS solution including (a) alizari yellow GG and (b)
110 chrome yellow under the on-off operation of the UV light is shown; (a) 120 s after the UV irradiation,
111 (b), (c), and (d) correspond to 120, 240 and 480 s after the UV was turned on.

112

113 Raman microscopy was used for the characterization of the photo-generated crystals inside the
114 LC droplet. The crystal inside the 5CB droplet was measured under the same experimental conditions
115 in the formation of this object. Pure 5CB in the LC phase, pure *p*-nitrophenol (powder), and an SDS
116 solution with *p*-nitrophenol were measured for comparison (Fig.4). The Raman peaks of 420.9, 646.6,
117 789.2, 820.1, 838.7 and 1033.5 cm^{-1} correspond for 5CB and 874.4 and 1129.0 cm^{-1} were for *p*-

nitrophenol. Obviously, the mixture spectra of 5CB and *p*-nitrophenol were observed for the droplet including the photo-generated crystal, which was assigned as *p*-nitrophenol. The Raman spectrum was not obtained for *p*-nitrophenol solved in an SDS solution under the same experimental condition. At this moment, we could not exclude the possibility of the formation of co-crystal of 5CB and *p*-nitrophenol,[31] but we suppose that it is low considering this could happen for several different chemicals.

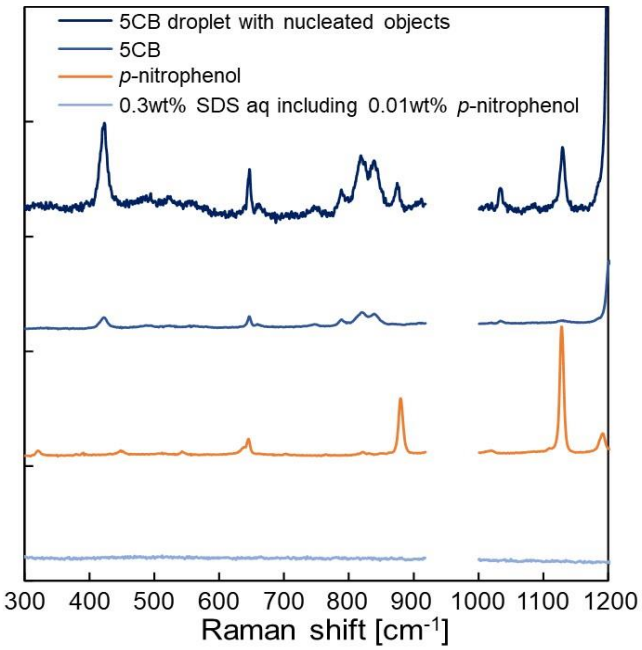

Fig.4 The Raman spectrum of a photo-generated crystal in a 5CB droplet (top). The Raman spectra for pure 5CB, *p*-nitrophenol (powder), and a 0.3wt% SDS solution with 0.01wt% *p*-nitrophenol are shown for comparison. The spectral region from 920-1000 cm^{-1} was removed due to the noise of the excitation light source.

It is noted that the chemical source formed inside the droplet was initially dissolved in the outer

131 solution. The temporal change of the UV/Vis absorption spectrum of the outer solution was measured
132 during the UV irradiation to investigate the chemical resource. A single 5CB droplet with a volume of
133 20 μL was prepared in a 0.3wt% SDS solution with 0.001wt% *p*-nitrophenol (10 mL) in a vial. The
134 outer SDS solution was sampled with 0.5 mL every 30 seconds during the UV irradiation, and the
135 absorbance of each sample was measured by UV/Vis spectrometer.

136 The spectra for the different sampling times during the UV light irradiation are shown in Fig.5.
137 The absorption peak at 316 nm for *p*-nitrophenol (Fig.S2) gradually decreased during the UV
138 irradiation. This result indicates that the amount of *p*-nitrophenol in the outer SDS solution was
139 decreased during the light irradiation. This result supports that the dyes migrated from the outer
140 solution into the LC droplet, which was the source of the nucleated crystal.

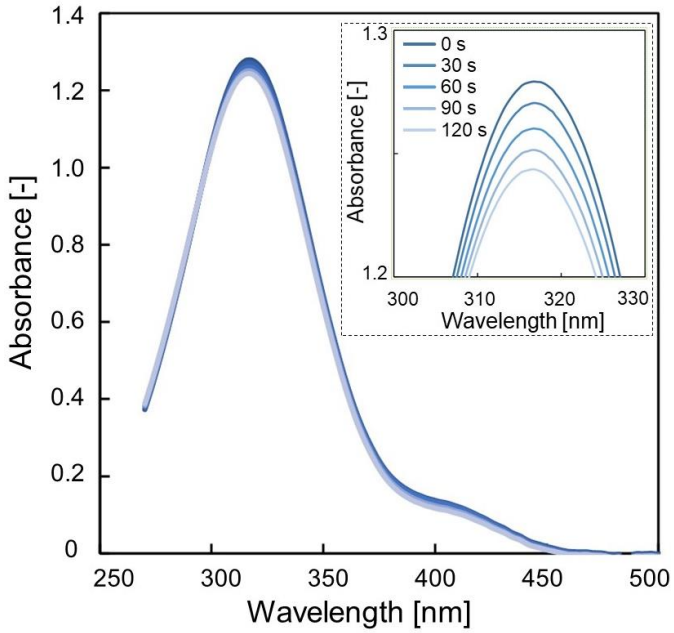

141 Fig.5 The temporal change of the UV/Vis absorption spectra for the outside SDS solution with *p*-
142 nitrophenol (0.001 %), including an 5CB droplet during the UV light irradiation. The outside solution
143 was sampled every 30 second during the UV light irradiation.

The interfacial tension was monitored during the light irradiation to obtain further evidence of the exchange of the dye molecules at the interface between the LC droplet and the SDS solution. The interfacial tension change during the on-off operation of the UV light was monitored by the pendant drop measurement for the LC droplet in an SDS solution with *p*-nitrophenol (Fig.6). The UV light was irradiated for 20 seconds twice. The interfacial tension gradually increased during the UV irradiation and decreased after being turned off. This result indicates the desorption of molecules from the LC/water interface during the UV irradiation. This desorption process is interpreted by the desorption of the dyes initially adsorbed at the LC/water interface into the LC phase.

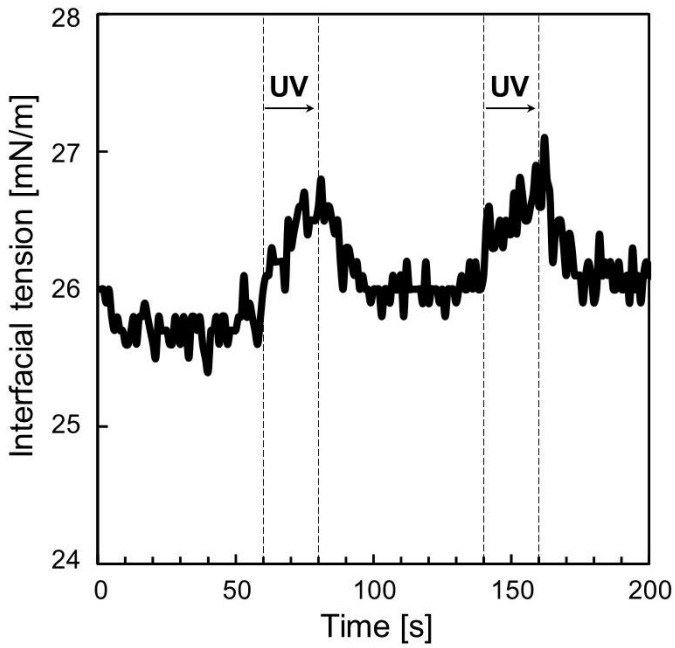

Fig.6 The change of the interfacial tension during the on-off operation of the UV light for a 5CB droplet in an SDS solution with *p*-nitrophenol (0.01 wt%). The UV light was irradiated twice for 20 seconds at 60 and 140 seconds during the measurement.

156

157 The interfacial tension monitoring suggested the dye desorption was promoted from the
158 interface by light, which indicates that the dyes were initially adsorbed at the LC/water interface. The
159 contact angle of an LC droplet on the dye concentration in the outer solution was studied to verify it.
160 A drop of 5CB with a volume of 20 μL was dropped onto a hydrophobically-treated petri-dish. The
161 contact angles of the 5CB droplets surrounded by 0.3wt% SDS solutions (0, 0.1, and 0.5 wt% *p*-
162 nitrophenol) were measured. The pictures of each droplet are shown in Fig.S1 in SI. The contact angle
163 decreased as the dye concentration in the outer solution increased. This result indicates the dyes adsorb
164 at the interface in a static state, supporting our assumption.

165 There is still a mystery on the mechanism of the dye solubilization into the LC droplet. Organic
166 molecules dissolved in an aqueous surfactant solution are usually solubilized into the organic phase
167 as a reverse micelle. The SDS molecules could make a reverse micelle of the dyes and promote
168 solubilization into the LC phase. The effect of the reverse micellar solubilization was studied by
169 changing the type of the surfactants. Instead of SDS, we used polyvinyl alcohol (PVA) as a protecting
170 agent for the LC droplet. The PVA could keep the stability of the LC droplet interface by a random
171 coil formation but does not make a reverse micelle for the dyes.[29] A 5CB droplet was prepared in a
172 PVA solution (1 wt%) with 0.01wt% *p*-nitrophenol, and the UV light was illuminated similarly. The
173 result is shown in Fig. 7 (Movie S4 in SI). The nucleation of small objects started inside the LC droplet

about 30 s after the UV light irradiation, which was similar to the SDS solution. This result indicates that the reverse micellar solubilization was not a necessary process for transferring the dye molecules into the LC phase, and it is assumed that they were injected into the LC phase on their own.

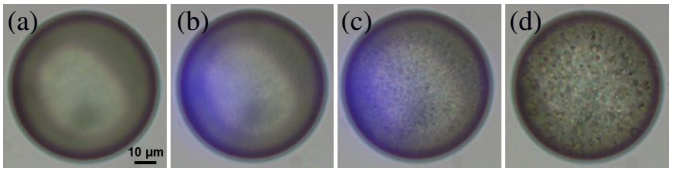

Fig.7 The snapshots of the 5CB droplet in a PVA solution with *p*-nitrophenol (0.01 wt%) under the UV on-off operation is shown. (a) before UV irradiation (b) and (c) 30 s, 90 s after the UV light turned on, (d) 60 s after the UV light turned off.

From this experiment, we had more important information on this crystallization process. As we could confirm from Movie S4 and Fig.7, the small nuclei did not approach the droplet center, even though the dye nucleation was induced in a PVA solution, too. The nucleated and grown small objects kept fluctuating inside the LC droplet. Since PVA imposes the planer orientation of the LC molecules (parallel) at the LC/solution interface, the LC alignment in the droplet becomes bipolar configuration, where two topological defects are formed at each pole and do not have one in the center.[12,29] This result strongly suggests that the topological defect at the center or the radial alignment of the LC droplet has a crucial role in the build-up of the crystalline phase.

The effect of the LC phase on the nuclei formation was investigated from the observation of the oil droplet behavior (toluene droplet) under the same experimental condition. (Movie S5 in SI).

No reactions proceeded during the light irradiation. This result indicates that the LC phase was necessary for taking up the dyes into the LC phase or for the nucleation itself. Furthermore, we investigated the temperature influence for the crystallization because the photo-absorbed dyes release heat via photothermal relaxation and/or photo-isomerization in the case of azo-dyes. The behavior of the 5CB droplet in an SDS solution with *p*-nitrophenol was observed under the temperature variation in a temperature-controlled vessel. The sample temperature was initially set at room temperature (25°C), and it was raised by 5 °C, which is sufficiently higher than the calculated temperature rise due to the photo-absorption of *p*-nitrophenol (~0.8°C), and was lowered to the room temperature again. (Movie S6 in SI). No reaction was observed, and only the focus point was defocused under the temperature variation. This result indicates that photo-excitation has a role in the crystallization process, possibly for being taken up into the LC phase.

Based on the observations and considerations, we propose the following possible crystallization mechanism. It is supposed that a part of dye molecules was initially adsorbed at the LC/water interface, confirmed from the interfacial tension dependence on the dye concentration. Based on the dynamic interfacial tension measurement, the desorption of these dyes into the LC phase was promoted during the UV light irradiation. Also, the dyes could be provided from the outside solution. The process gradually would increase the concentration of the dyes inside the LC droplet. We could not figure out why the dye injection into the LC phase was triggerd by light irradiation, but

one of the possibilities is that the photo-induced dipole (excited state) prefers the molecularly oriented environment like LC. This intake could be a similar process as the gold nanorods with a large dipole moment were taken and aligned by LCs to show a long-range ordering.[16] This should be studied in more detail on the molecular properties of dyes and LCs based on the molecular dynamics. Overcoming the saturation concentration of the dyes, they start to form nuclei at random positions. Then, the nuclei gathered to the topological defect at the center and grew with a branched shape. The accumulation of objects to the LC defects (dislocation) was previously observed,[13,17,18] where a preferable environment for assembly of objects is provided by reducing the high free energy core of the LC defects.[13] In our case, the nuclei were collected at the point defect at the center. The object can keep the crystalline phase confirmed by the crossed-Nicole observation, and this suggests that the LC provided a preferable environment for molecular orientation suitable for the crystal growth. It was reported for pure LC molecules that the LC phase could work as a metastable state, inducing frustration for the crystal formation. The LC phase could potentially ease the nucleation of molecules by the ordering environment for extraneous molecules,[28] and it would be a similar concept to the crystal sponge.[6]

Conclusion

We found a photo-controllable unique crystallization process at the topological defect of an

LC droplet in a surfactant solution with dye molecules. The dye molecules, initially adsorbed at the interface of the droplet/surfactant solution, were desorbed into the LC droplet during the light irradiation. The dye molecules overcame the saturated concentration inside the LC droplet, starting to form crystal nuclei at random positions. These crystals gathered to the topological defect, growing with a branched shape in a crystalline form. This process was demonstrated for several different dyes with the light absorption matching the irradiated light source. This is a brand-new crystallization technique, and controllable by light, and also showed another interesting property of topological defects. This methodology is a simple and easy method for crystallization and could crystallize various molecules for pharmaceutical purposes and structural analyses for biomolecules.

Methods

LC droplets were prepared using a microfluidic device. A schematic drawing of the device is shown in Fig. S2 in SI, and the detailed method was described. The typical size of the droplets was 50 μm in diameter.

4-cyano-4'-pentylbiphenyl (5CB, nematic phase: 22.5 - 35 °C) was used as an inner fluid and an LC material (Fig.8(a)). A sodium dodecyl sulfate (SDS, 0.3wt%, 25°C) solution was used as an outer fluid. The solution included water-soluble dyes whose absorption wavelengths have an overlap at 365 nm, corresponding to the UV-LED wavelength. The dyes were *p*-nitrophenol, alizarin yellow GG, and chrome yellow, as their molecular structures are shown in Fig.8(b), (c), and (d), respectively. These absorption spectra for them are shown in Fig.S3 in SI. The schematic drawing of the observation setup is shown in Fig.S4 in SI. The droplet behavior was observed by an inverted microscope with a UV light illumination from the top side.

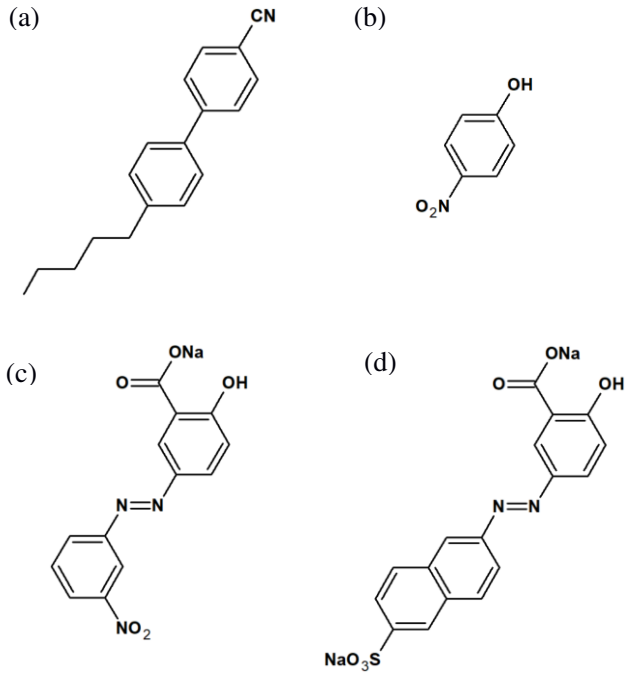

Fig.8 The molecular structures of the LC and the dye molecules. The dyes were dissolved in a surfactant solution. (a) 4-cyano-4'-pentylbiphenyl (5CB) (b) *p*-nitrophenol (c) alizarin yellow GG (d) chrome yellow.

Raman microscopy (Lamda Vision) was used for the characterization of chemicals inside the droplets. The excitation laser has a wavelength of 532 nm (MLL-III-532) with an intensity of 30 mW.

The pendant drop method (DMs-401, Kyowa Kaimen Kagaku) was utilized to monitor the interfacial tension for an LC droplet in a solution. The sample was prepared by preparing a pendant drop (15 μL) of 5CB from a syringe needle into a measurement cell filled with an SDS solution with dye molecules. The image sequence of the pendant drop was acquired by a camera every second, and each interfacial tension was calculated from the droplet shape by fitting with the Young-Laplace equation.

Acknowledgments

This research was supported by the Institute of Science and Engineering, Chuo University.

Author contributions

Y. S. and K. K. designed the experiments and analyzed results, and wrote the paper.

Competing interests

The authors declare no competing interests.

Additional information

Supplementary information is available for this paper at ???.

References

1. LaMer, V. K. & Dinegar, R. H. Theory, Production and Mechanism of Formation of Monodispersed Hydrosols. *J. Am. Chem. Soc.* **72**, 4847–4854 (1950).

2. Gao, Z., Rohani, S., Gong, J. & Wang, J. Recent Developments in the Crystallization Process: Toward the Pharmaceutical Industry. *Engineering* **3**, 343–353 (2017).

3. Yang, Y. & Nagy, Z. K. Advanced control approaches for combined cooling/antisolvent crystallization in continuous mixed suspension mixed product removal cascade crystallizers. *Chemical Engineering Science* **127**, 362–373 (2015).

4. Alvarez, A. J. & Myerson, A. S. Continuous Plug Flow Crystallization of Pharmaceutical Compounds. *Crystal Growth & Design* **10**, 2219–2228 (2010).

5. McGlone, T. *et al.* Oscillatory Flow Reactors (OFRs) for Continuous Manufacturing and Crystallization. *Org. Process Res. Dev.* **19**, 1186–1202 (2015).

6. Hoshino, M., Khutia, A., Xing, H., Inokuma, Y. & Fujita, M. The crystalline sponge method updated. *IUCrJ* **3**, 139–151 (2016).

7. Inokuma, Y. *et al.* X-ray analysis on the nanogram to microgram scale using porous complexes. *Nature* **495**, 461–466 (2013).

8. Mitov, M. Cholesteric liquid crystals in living matter. *Soft Matter* **13**, 4176–4209 (2017).

9. Nersisyan, S. R. & Tabiryan, N. V. Polarization Imaging Components Based on Patterned Photoalignment. *Molecular Crystals and Liquid Crystals* **489**, 156/[482]-168/[494] (2008).

10. Nersisyan, S., Tabiryan, N., Steeves, D. M. & Kimball, B. R. Fabrication of liquid crystal polymer axial waveplates for UV-IR wavelengths. *Opt. Express, OE* **17**, 11926–11934 (2009).

11. Wu, H. *et al.* Arbitrary photo-patterning in liquid crystal alignments using DMD based lithography system. *Opt. Express* **20**, 16684–16689 (2012).

12. Lopez-Leon, T. & Fernandez-Nieves, A. Drops and shells of liquid crystal. *Colloid Polym Sci* **289**, 345–359 (2011).

13. Wang, X., Miller, D. S., Bukusoglu, E., de Pablo, J. J. & Abbott, N. L. Topological defects in liquid crystals as templates for molecular self-assembly. *Nature Materials* **15**, 106–112 (2016).

14. Kawaguchi, K., Kageyama, R. & Sano, M. Topological defects control collective dynamics in neural progenitor cell cultures. *Nature* **545**, 327–331 (2017).

15. Saw, T. B. *et al.* Topological defects in epithelia govern cell death and extrusion. *Nature* **544**, 212–216 (2017).

16. Liu, Q. *et al.* Self-Alignment of Plasmonic Gold Nanorods in Reconfigurable Anisotropic Fluids for Tunable Bulk Metamaterial Applications. *Nano Lett.* **10**, 1347–1353 (2010).

17. Milette, J. *et al.* Reversible long-range patterning of gold nanoparticles by smectic liquid crystals. *Soft Matter* **8**, 6593–6598 (2012).

18. Coursault, D. *et al.* Linear Self-Assembly of Nanoparticles Within Liquid Crystal Defect Arrays. *Advanced Materials* **24**, 1461–1465 (2012).

19. Pires, D., Fleury, J.-B. & Galerne, Y. Colloid Particles in the Interaction Field of a Disclination Line in a Nematic Phase. *Phys. Rev. Lett.* **98**, 247801 (2007).

20. Wood, T. A., Lintuvuori, J. S., Schofield, A. B., Marenduzzo, D. & Poon, W. C. K. A Self-Quenched Defect Glass in a Colloid-Nematic Liquid Crystal Composite. *Science* **334**, 79–83 (2011).

21. Tkalec, U., Ravnik, M., Čopar, S., Žumer, S. & Muševič, I. Reconfigurable Knots and Links in Chiral Nematic Colloids. *Science* **333**, 62–65 (2011).

22. Jin, C., Krüger, C. & Maass, C. C. Chemotaxis and autochemotaxis of self-propelling droplet swimmers. *PNAS* **114**, 5089–5094 (2017).

23. Herminghaus, S. *et al.* Interfacial mechanisms in active emulsions. *Soft Matter* **10**, 7008–7022 (2014).

24. Krüger, C., Bahr, C., Herminghaus, S. & Maass, C. C. Dimensionality matters in the collective behaviour of active emulsions. *Eur. Phys. J. E* **39**, 64 (2016).

25. Sakai, Y., Sohn, W. Y. & Katayama, K. Optical motion control of liquid crystalline droplets by host–guest molecular interaction. *Soft Matter* **15**, 7159–7165 (2019).

26. Dogishi, Y., Sakai, Y., Sohn, W. Y. & Katayama, K. Optically induced motion of liquid crystalline droplets. *Soft Matter* **14**, 8085–8089 (2018).

27. Sakai, Y., Sohn, W. Y. & Katayama, K. Photo-controllable rotational motion of cholesteric liquid

crystalline droplets in a dispersion system. *RSC Adv.* **10**, 21191–21197 (2020).

28. Syme, C. D. *et al.* Frustration of crystallisation by a liquid–crystal phase. *Scientific Reports* **7**, 42439 (2017).

29. Wang, D., Park, S.-Y. & Kang, I.-K. Liquid crystals: emerging materials for use in real-time detection applications. *J. Mater. Chem. C* **3**, 9038–9047 (2015).

30. Prishchepa, O. O., Shabanov, A. V. & Zyryanov, V. Y. Director configurations in nematic droplets with inhomogeneous boundary conditions. *Phys Rev E Stat Nonlin Soft Matter Phys* **72**, 031712 (2005).

31. Bushuyev, O. S., Friščić, T. & Barrett, C. J. Controlling Dichroism of Molecular Crystals by Cocrystallization. *Crystal Growth & Design* **16**, 541–545 (2016).

Figure captions

FIG.1 The snapshots of a 5CB droplet in an SDS solution with *p*-nitrophenol (0.01 wt%) under the on-off operation of the UV light is shown; (a) before irradiation, (b) - (e) 0, 30, 60 and 90 s after the UV was turned on, (f) - (h) 0, 60, and 120 s after the UV light was turned off, (i) and (j) 0 and 30 s after the UV light was turned on again.

FIG.2 The snapshots of the 5CB droplet in an SDS solution with *p*-nitrophenol (0.01 %) observed by the polarization microscope under the crossed Nicole condition; (a) before irradiation (b) after the UV irradiation for 60 s. The white arrow in (a) indicates the direction of the analyzer and the polarizer.

FIG. 3 The snapshots of the 5CB droplet in an SDS solution including (a) alizari yellow GG and (b) chrome yellow under the on-off operation of the UV light is shown; (a) 120 s after the UV irradiation, (b), (c), and (d) correspond to 120, 240 and 480 s after the UV was turned on.

FIG. 4 The Raman spectrum of a photo-generated crystal in a 5CB droplet (top). The Raman spectra for pure 5CB, *p*-nitrophenol (powder), and a 0.3wt% SDS solution with 0.01wt% *p*-nitrophenol are shown for comparison. The spectral region from 920-1000 cm^{-1} was removed due to the noise of the excitation light source.

FIG. 5 The temporal change of the UV/Vis absorption spectra for the outside SDS solution with *p*-nitrophenol (0.001 %). An 5CB droplet was included in the solution, and the outside solution was sampled every 30 second during the UV light irradiation.

FIG.6 The change of the interfacial tension during the on-off operation of the UV light for a 5CB droplet in a SDS solution with *p*-nitrophenol (0.01 wt%). The UV light was irradiated twice for 20 seconds at 60 and 140 seconds during the measurement.

FIG 7. The snapshots of the 5CB droplet in an PVA solution with *p*-nitrophenol (0.05 wt%) under the UV on-off operation is shown. (a) before UV irradiation (b) and (c) 30 s, 90 s after the UV light turned on, (d) 60 s after the UV light turned off.

FIG 8. The molecular structures of the LC and the dye molecules. The dyes were dissolved in a surfactant solution. (a) 4-cyano-4'-pentylbiphenyl (5CB) (b) *p*-nitrophenol (c) alizarin yellow GG (d) chrome yellow.

Figures

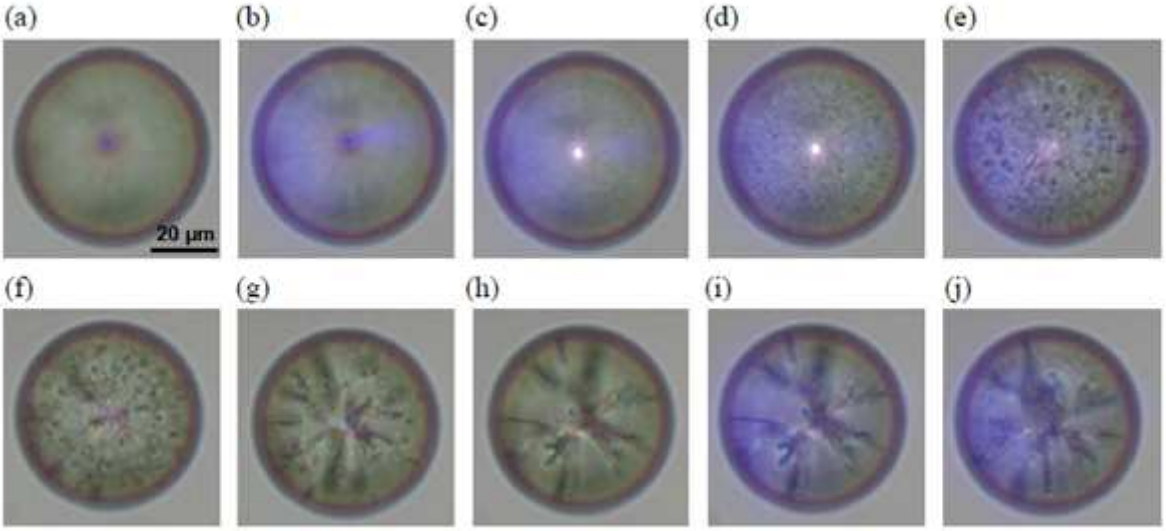

Figure 1

The snapshots of a 5CB droplet in an SDS solution with p-nitrophenol (0.01 wt%) under the on-off operation of the UV light is shown; (a) before irradiation, (b) - (e) 0, 30, 60 and 90 s after the UV was turned on, (f) - (h) 0, 60, and 120 s after the UV light was turned off, (i) and (j) 0 and 30 s after the UV light was turned on again.

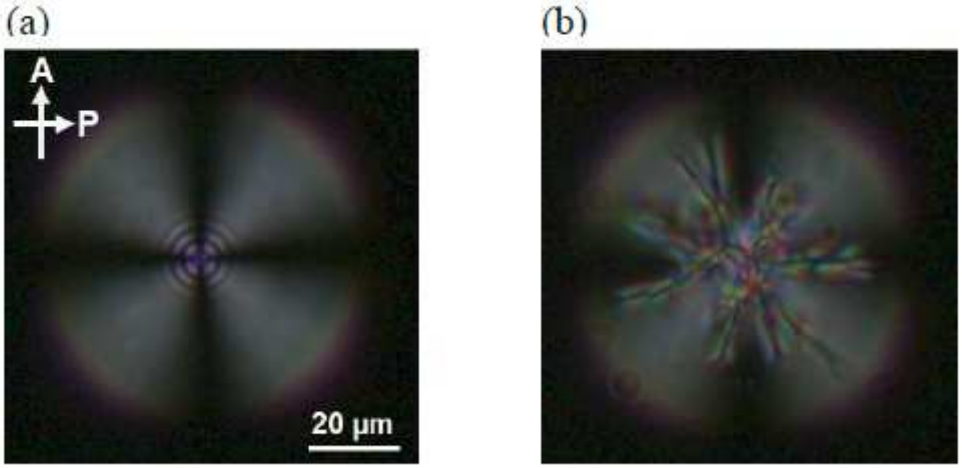

Figure 2

The snapshots of the 5CB droplet in an SDS solution with p-nitrophenol (0.01 %) observed by the polarization microscope under the crossed Nicole condition; (a) before irradiation (b) after the UV irradiation for 60 s. The white arrow in (a) indicates the direction of the analyzer and the polarizer.

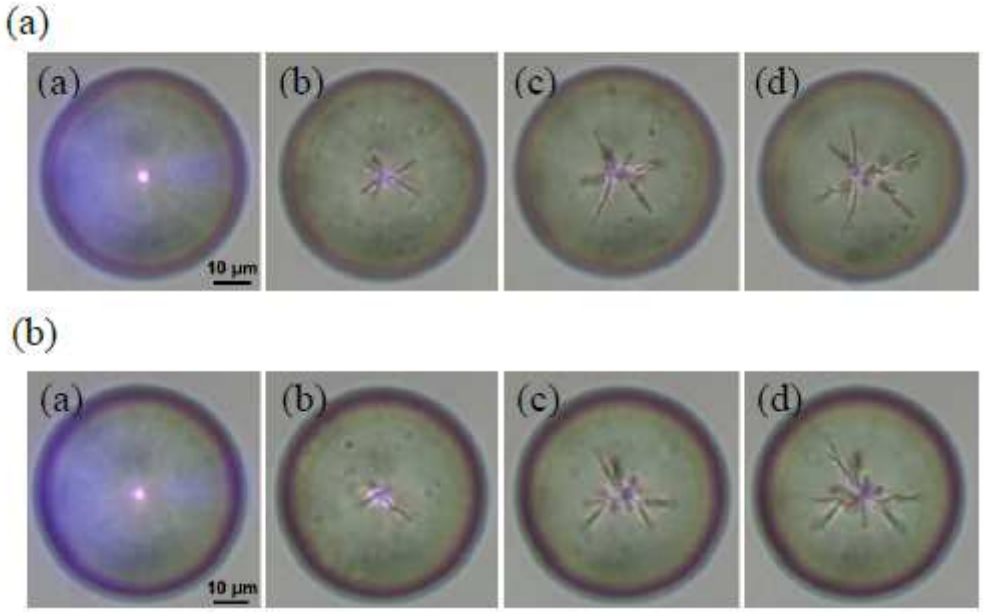

Figure 3

The snapshots of the 5CB droplet in an SDS solution including (a) alizari yellow GG and (b) chrome yellow under the on-off operation of the UV light is shown; (a) 120 s after the UV irradiation, (b), (c), and (d) correspond to 120, 240 and 480 s after the UV was turned on.

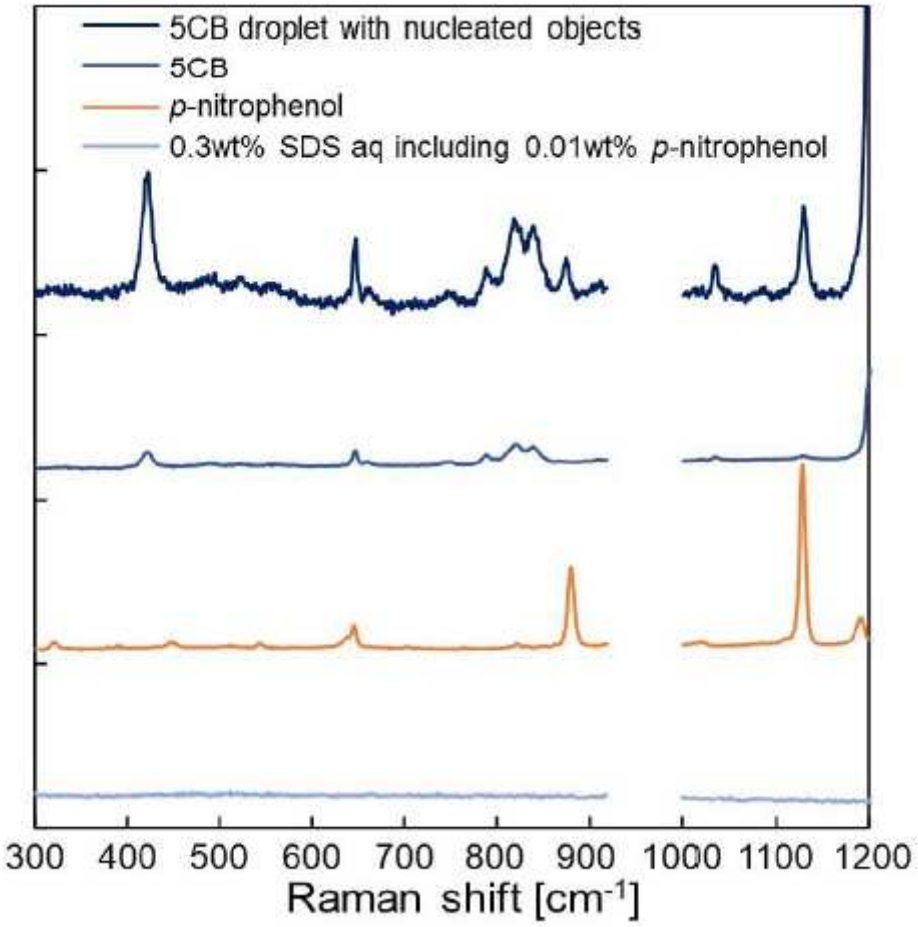

Figure 4

The Raman spectrum of a photo-generated crystal in a 5CB droplet (top). The Raman spectra for pure 5CB, p-nitrophenol (powder), and a 0.3wt% SDS solution with 0.01wt% p-nitrophenol are shown for comparison. The spectral region from 920-1000 cm-1 was removed due to the noise of the excitation light source.

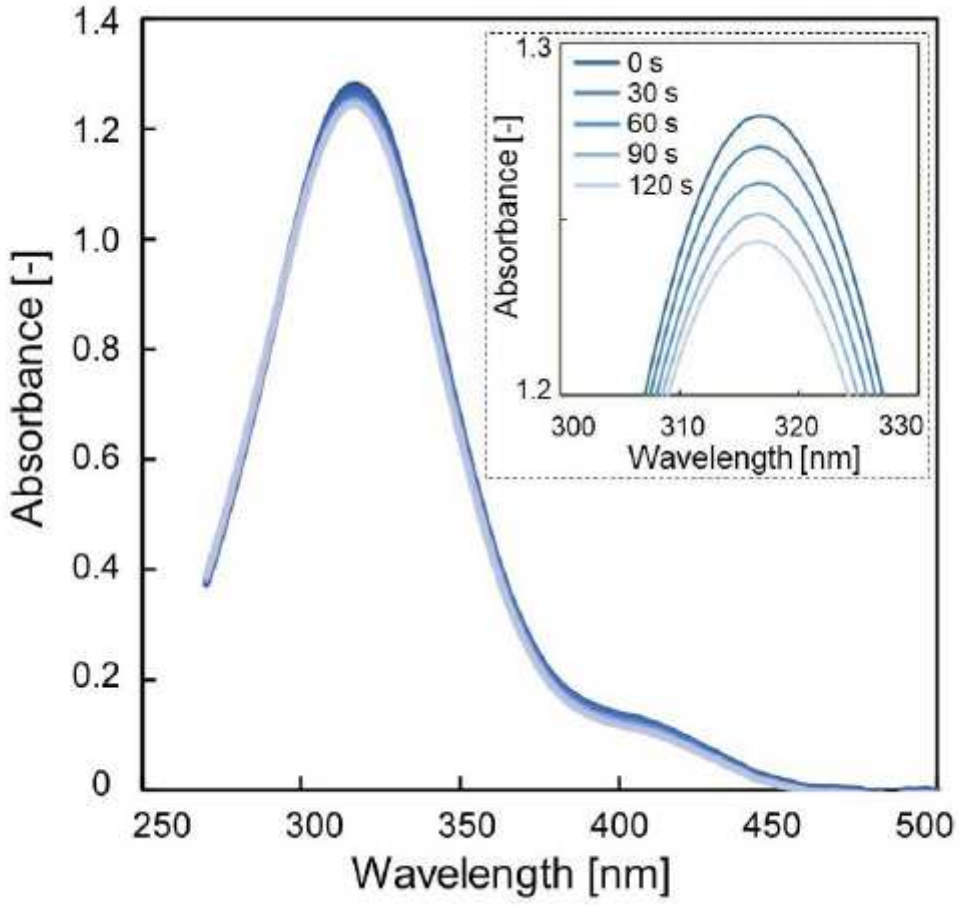

Figure 5

The temporal change of the UV/Vis absorption spectra for the outside SDS solution with p- nitrophenol (0.001 %). An 5CB droplet was included in the solution, and the outside solution was sampled every 30 second during the UV light irradiation.

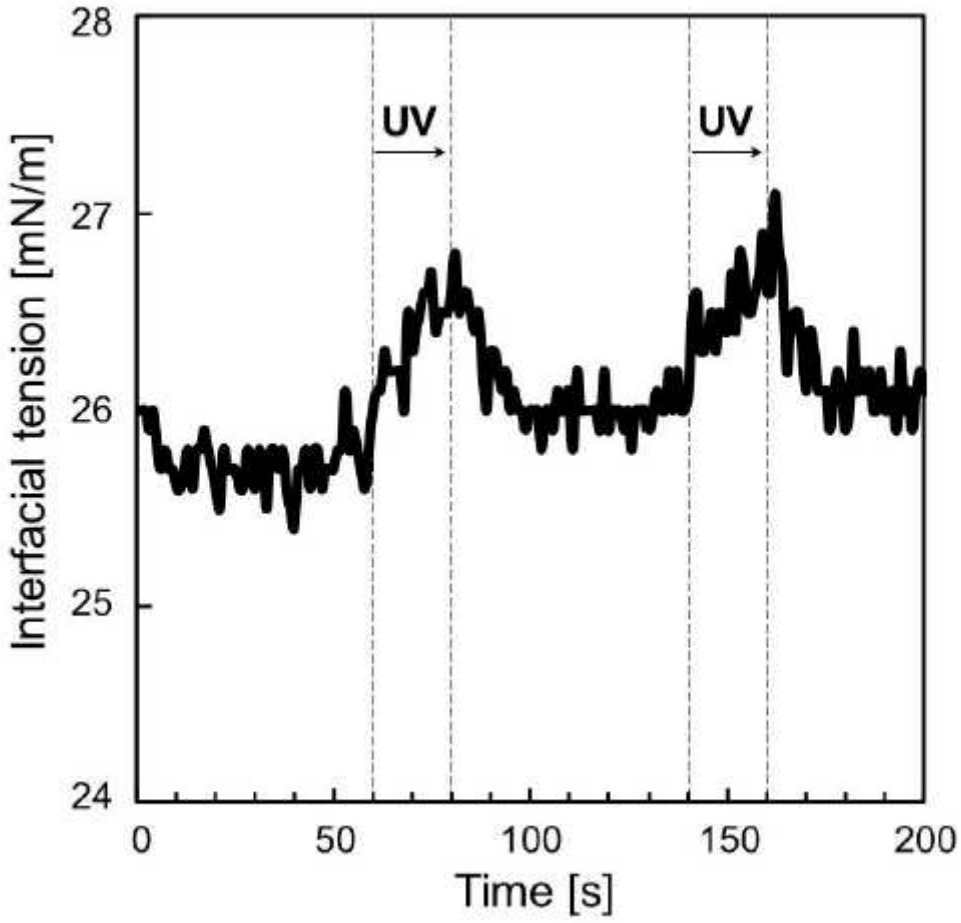

Figure 6

The change of the interfacial tension during the on-off operation of the UV light for a 5CB droplet in a SDS solution with p-nitrophenol (0.01 wt%). The UV light was irradiated twice for 20 seconds at 60 and 140 seconds during the measurement.

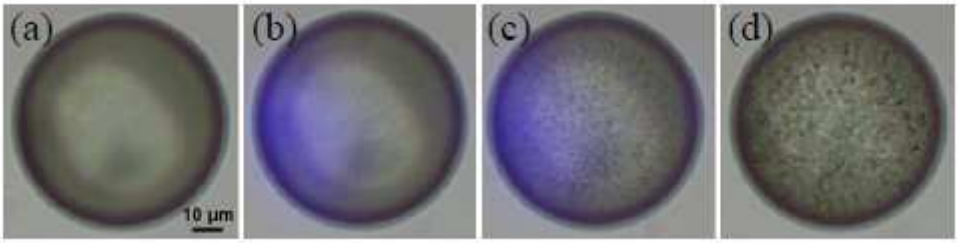

Figure 7

The snapshots of the 5CB droplet in an PVA solution with p-nitrophenol (0.05 wt%) under the UV on-off operation is shown. (a) before UV irradiation (b) and (c) 30 s, 90 s after the UV light turned on, (d) 60 s after the UV light turned off.

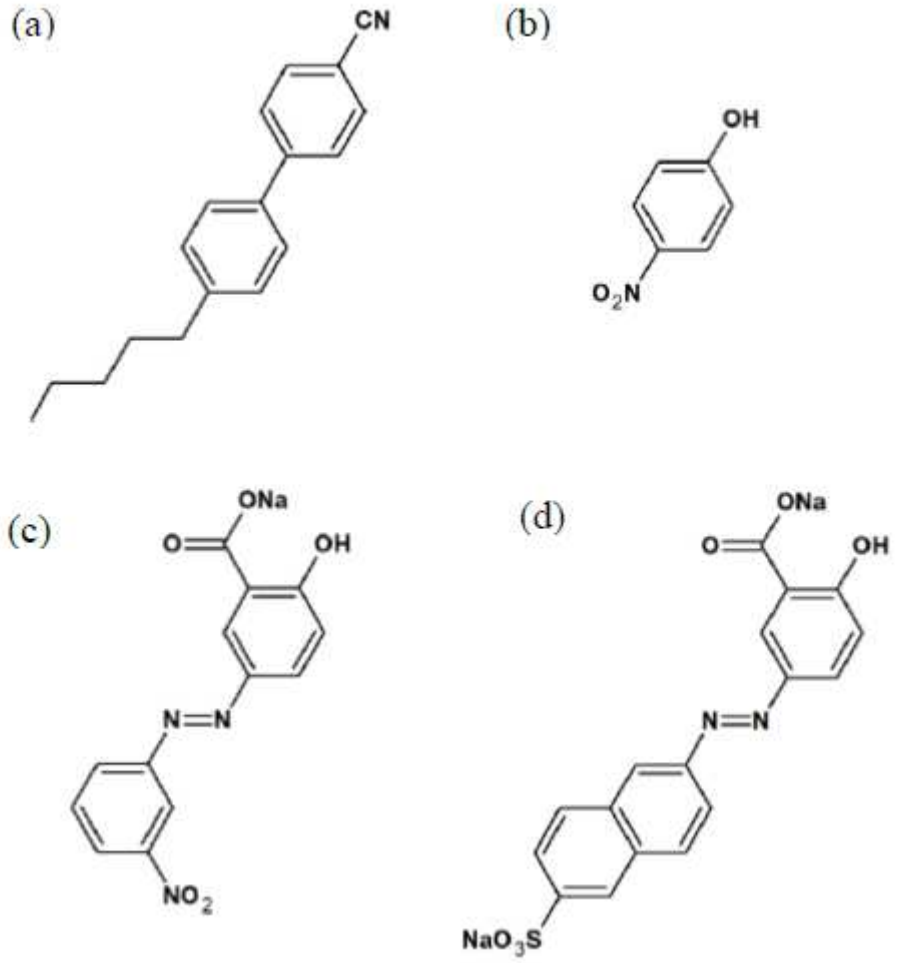

Figure 8

The molecular structures of the LC and the dye molecules. The dyes were dissolved in a surfactant solution. (a) 4-cyano-4’-pentylbiphenyl (5CB) (b) p-nitrophenol (c) alizarin yellow GG (d) chrome yellow

Supplementary Files

This is a list of supplementary files associated with this preprint. Click to download.

- 20210215Supportinginformation.pdf
- MovieS45CBdropletPVApnitrophenol.mp4
- MovieS3a5CBdropletSDSalizarinyellow.mp4
- MovieS3b5CBdropletSDSchromeyellow.mp4
- MovieS65CBdropletSDSpnitorphenolheater.mp4
- MovieS5toluenedropletSDSpnitrophenol.mp4
- MovieS25CBdropletSDSpnitrophenolcrossnicole.mp4

- MovieS15CBdropletSDSpnitrophenol.mp4